CXC-Chemokine Receptor 4 Antagonist AMD3100 Promotes Cardiac Functional Recovery After Ischemia/Reperfusion Injury via Endothelial Nitric Oxide Synthase–Dependent Mechanism

Kentaro Jujo, MD, PhD; Masaaki Ii, MD, PhD; Haruki Sekiguchi, MD, PhD; Ekaterina Klyachko, BS; Sol Misener, BS; Toshikazu Tanaka, MD; Jörn Tongers, MD, PhD; Jérôme Roncalli, MD, PhD; Marie-Ange Renault, PhD; Tina Thorne, BS; Aiko Ito, BS; Trevor Clarke, BS; Christine Kamide, BS; Yukio Tsurumi, MD, PhD; Nobuhisa Hagiwara, MD, PhD; Gangjian Qin, MD, PhD; Michio Asahi, MD, PhD; Douglas W. Losordo, MD

Background—CXC-chemokine receptor 4 (CXCR4) regulates the retention of stem/progenitor cells in the bone marrow (BM), and the CXCR4 antagonist AMD3100 improves recovery from coronary ligation injury by mobilizing stem/progenitor cells from the BM to the peripheral blood. Thus, we investigated whether AMD3100 also improves recovery from ischemia/reperfusion injury, which more closely mimics myocardial infarction in patients, because blood flow is only temporarily obstructed.

Methods and Results—Mice were treated with single subcutaneous injections of AMD3100 (5 mg/kg) or saline after ischemia/reperfusion injury. Three days later, histological measurements of the ratio of infarct area to area at risk were smaller in AMD3100-treated mice than in mice administered saline, and echocardiographic measurements of left ventricular function were greater in the AMD3100-treated mice at week 4. $CXCR4^+$ cells were mobilized for just 1 day in both groups, but the mobilization of $sca1^+/flk1^+$ cells endured for 7 days in AMD3100-treated mice compared with just 1 day in the saline-treated mice. AMD3100 upregulated BM levels of endothelial nitric oxide synthase (eNOS) and 2 targets of eNOS signaling, matrix metalloproteinase-9 and soluble Kit ligand. Furthermore, the loss of BM eNOS expression abolished the benefit of AMD3100 on $sca1^+/flk1^+$ cell mobilization without altering the mobilization of $CXCR4^+$ cells, and the cardioprotective effects of AMD3100 were retained in eNOS-knockout mice that had been transplanted with BM from wild-type mice but not in wild-type mice with eNOS-knockout BM.

Conclusions—AMD3100 prolongs BM progenitor mobilization and improves recovery from ischemia/reperfusion injury, and these benefits appear to occur through a previously unidentified link between AMD3100 and BM eNOS expression. **(*Circulation.* 2013;127:63-73.)**

Key Words: ischemia ■ myocardium ■ nitric oxide synthase ■ pharmaceutical preparations ■ reperfusion

In response to ischemic myocardial injury, stem/progenitor cells are mobilized from the bone marrow (BM) to the peripheral blood (PB) and become incorporated into the injured tissue, where a subset of the mobilized cells, including endothelial progenitor cells (EPCs), contribute to cardiac recovery by enhancing vessel growth.[1–3] Before mobilization, progenitor cells are sequestered in the BM by interactions between CXC chemokine receptor 4 (CXCR4) and stromal-cell–derived factor 1 (SDF-1).[4,5] Mobilization is triggered when this interaction is disrupted, and SDF-1 expression in the ischemic tissue contributes to the recruitment and incorporation of mobilized EPCs.[6] SDF-1 also induces the migration of EPCs in vitro,[7] and SDF-1–CXCR4 signaling appears to influence EPC proliferation and survival.[8,9] Thus, the SDF-1/CXCR4 axis is a key regulator of the activity of stem/progenitor cells, including EPCs, particularly the release from BM and the retention/recruitment of progenitors in/to ischemic tissue.

Editorial see p 13
Clinical Perspective on p 73

CXCR4 also facilitates cellular entry of the human immunodeficiency virus, which prompted the development of

Received February 10, 2012; accepted October 26, 2012

From the Feinberg Cardiovascular Research Institute, Feinberg School of Medicine, Northwestern University, Chicago, IL (K.J., E.K., S.M., T.T., J.T., J.R., M.-A.R., T.T., A.I., T.C., C.K., G.Q., D.W.L.); Department of Cardiology, Tokyo Women's Medical University, Tokyo, Japan (K.J., H.S., Y.T., N.H.); Department of Pharmacology, Faculty of Medicine, Osaka Medical College, Osaka, Japan (M.I., M.A.); and Department of Cardiology and Angiology, Hannover Medical School, Hannover, Germany (J.T.).

The online-only Data Supplement is available with this article at http://circ.ahajournals.org/lookup/suppl/doi:10.1161/CIRCULATIONAHA.112.099242/-/DC1.

Correspondence: Masaaki Ii, MD, PhD, Department of Pharmacology, Faculty of Medicine, Osaka Medical College, 2–7, Daigaku-machi, Takatsuki, Osaka, 569–8686, Japan. E-mail masa0331@mac.com

Circulation **is available at http://circ.ahajournals.org** **DOI: 10.1161/CIRCULATIONAHA.112.099242**

AMD3100, a pharmacological CXCR4 antagonist.[10–12] In early pharmacokinetic studies, a single intravenous dose of AMD3100 unexpectedly increased circulating white blood cell counts in healthy volunteers,[13] and subsequent reports indicate that AMD3100 rapidly mobilizes hematopoietic progenitor cells in both humans and mice by reversibly blocking the SDF-1–CXCR4 interaction.[13–16] Previously, we have shown that a single dose of AMD3100 after surgical ligation of the coronary artery[17] increases the mobilization of BM progenitor cells (BMPCs), which leads to a greater BMPC accumulation in infarcted tissue and to improvements in vascularity and myocardial performance; furthermore, the effect of AMD3100 on BMPC mobilization endured for >1 week. This is somewhat surprising because the half-life of AMD3100 in serum is just 2 to 3 hours and consequently the short-term activity of AMD3100 as a CXCR4 antagonist should dissipate within a day of administration. Here, we investigated whether AMD3100 also improves myocardial recovery after ischemia/reperfusion (IR) injury, which more closely resembles the clinical presentation of acute myocardial infarction, because blood flow is obstructed temporarily rather than permanently. We also compared the time course and signaling pathways involved in BMPC mobilization and those associated with mobilization of $CXCR4^+$ mononuclear cells (MNCs).

Methods

Injury Model and Treatment

All mice were obtained from The Jackson Laboratories. BM transplantation surgery and IR injury were performed as described previously[18–20] and as summarized in the online-only Data Supplement. Mice received a single subcutaneous injection of AMD3100 (5 mg/kg, 125 μg in 100 μL; Sigma-Aldrich) or an equal volume of saline immediately after surgery was complete. Area at risk (AAR) and infarct area were measured as described in the online-only Data Supplement. AAR was presented as a percentage of the area of the entire left ventricle (LV); the infarct area, as a percentage of the AAR.

Physiological Assessments of LV Function

Echocardiographic measurements were performed with a commercially available high-resolution echocardiographic system (VEVO 770, VisualSonics Inc). End-systolic and end-diastolic LV areas on the short-axis view were traced at the midpapillary muscle level according to the instruction of the echocardiographic program, and the following calculation was used for area fractional shortening (FS%): (diastolic LV area−systolic LV area)/diastolic LV area.

PB Cell Counts

Detailed information is provided in the online-only Data Supplement.

Histological and Immunofluorescent Assessments

Detailed information is provided in the online-only Data Supplement.

In Vitro Assessments With Cultured, BM-Derived EPCs

Detailed information is provided in the online-only Data Supplement.

Luciferase Reporter Assay

Detailed information is provided in the online-only Data Supplement.

Quantitative Real-Time Reverse Transcription–Polymerase Chain Reaction

Detailed information, including primer and probe sequences (Table I), is provided in the online-only Data Supplement.

Statistical Analysis

All values were expressed as mean±SEM. Comparisons among samples from different mice at single or multiple time points were evaluated by unpaired *t* test (bar graph). Comparisons among consecutive samples from identified mouse in a single group were evaluated by 1-way ANOVA with the Bonferroni post hoc test (line graph). Comparisons among consecutive samples from identified mouse in multiple groups were evaluated by 2-way ANOVA with the Bonferroni post hoc test (line graph; the factors are the groups and time). We applied the Bonferroni adjustment to both comparisons of the groups within each time point and comparisons of each time point and baseline within each group only when the data were collected from identical mouse at multiple time points. A 2-sided value of $P<0.05$ was considered statistically significant.

Results

The in vivo experiments for histological and echocardiographic analyses were performed separately. Therefore, the difference in sample sizes for each group is due to different series of experiments.

AMD3100 Treatment Reduces Infarct Size and Improves Cardiac Performance After IR Injury

IR injury was induced by surgically occluding the left anterior descending artery for 60 minutes, and AMD3100 (125 μg in 100 μL) or an equal volume of saline was injected subcutaneously immediately after surgery was complete. Infarct size and the AAR for infarction were evaluated 3 days after IR injury by briefly reoccluding the left anterior descending artery, perfusing the hearts with microspheres, and then staining sections of heart tissue with triphenyltetrazolium chloride (Figure 1A). Viable tissue was stained deep red; the infarcted region remained colorless; and the AAR was identified by the absence of microspheres. The size of the AAR was similar in both treatment groups (Figure 1B), but the infarcted regions were significantly smaller in AMD3100-treated mice than in mice administered saline (Figure 1C). AMD3100 treatment was also associated with significantly less apoptosis on day 3 (Figure 1D) and with significantly less fibrosis on day 28 (Figure 1E) after IR injury.

Cardiac function was measured before IR injury and 7, 14, and 28 days afterward via echocardiographic assessments of LV fractional shortening, LV systolic area, and LV diastolic area. Fractional shortening was significantly greater and LV systolic area was significantly smaller in mice administered AMD3100 than in saline-treated mice on days 14 and 28 after IR injury, whereas LV diastolic area did not differ significantly between groups at any time point (Figure 1F–1H and Tables II and III in the online-only Data Supplement). Collectively, the results from these

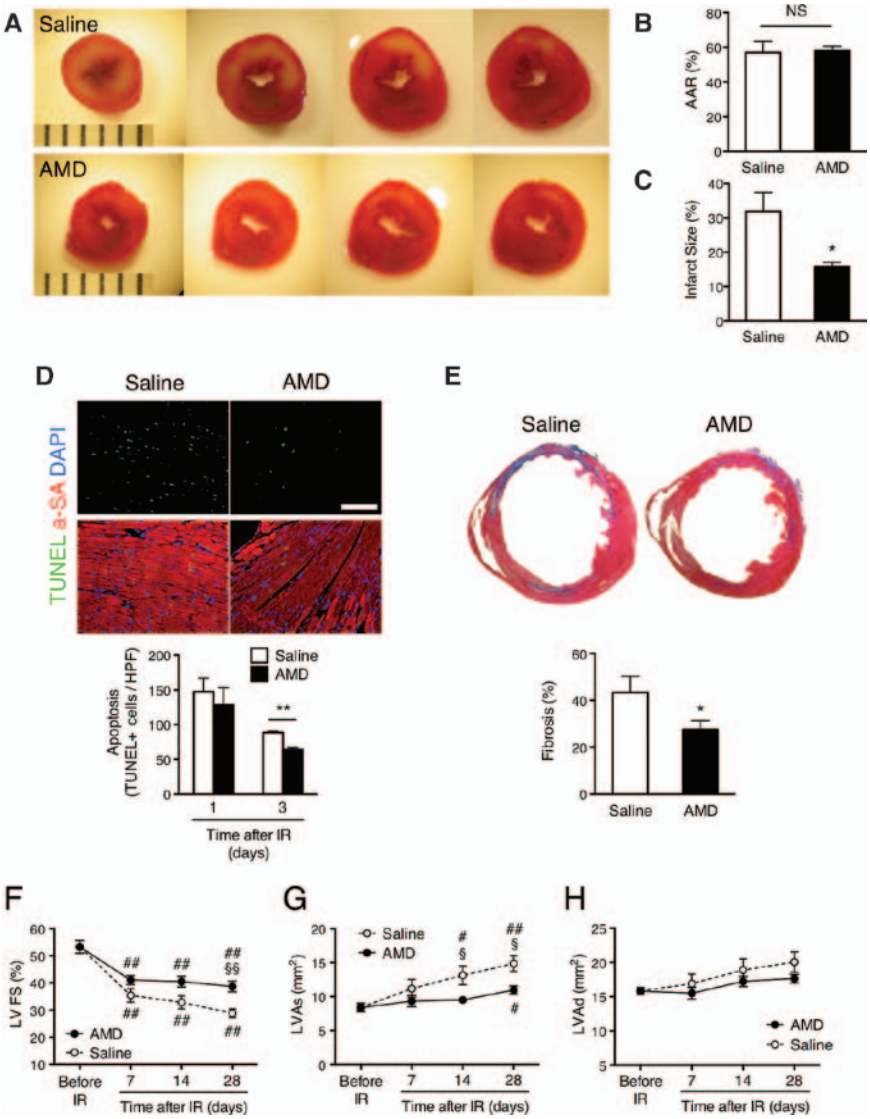

Figure 1. AMD3100 treatment improves cardiac function and reduces infarct size after ischemia/reperfusion (IR) injury. Mice were treated with saline alone or with 100 μL saline containing 125 μg AMD3100 after surgically induced IR injury. **A** through **C**, Area at risk (AAR) and infarct size were evaluated 3 days after IR injury via in vivo microsphere perfusion and triphenyltetrazolium chloride staining. **A**, Viable tissue stained deep red, and the infarcted region is colorless. Scale=1-mm increments. **B**, The AAR was identified by the absence of microspheres and is presented as a percentage of the total left ventricular (LV) area. **C**, Infarct size was normalized to the size of the AAR and presented as a percentage. **D**, Apoptosis was evaluated in terminal deoxynucleotidyl transferase dUTP nick-end labeling (TUNEL)–stained sections of heart tissue from mice euthanized 1 and 3 days after IR injury. Scale bar=100 μm. **E**, Fibrosis was evaluated in Masson trichrome–stained heart sections from mice euthanized 28 days after IR injury, quantified as the ratio of the length of fibrosis (blue) to the LV circumference, and presented as a percentage. **F** through **H**, Echocardiographic assessments of (**F**) LV fractional shortening (FS), (**G**) LV systolic area (LVAs), and (**H**) LV diastolic area (LVAd) were performed before IR injury and 7 to 28 days afterward; heart rates were maintained at 400 to 500 bpm via isoflurane inhalation. #*P*<0.05 and ##*P*<0.01 vs before injection; **B** and **C**, n=3 per treatment group; **D**, n=3 to 5 per treatment group; **E**, n=6 to 9 per treatment group; **F** through **H**, n=10 per treatment group at each time point. a-SA indicates α-sarcomeric actin; and HPF, high-power field. **P*<0.05, ***P*<0.01, §Bonferroni-adjusted *P*<0.05 and §§Bonferroni-adjusted *P*<0.01 vs saline.

histological and echocardiographic assessments suggest that a single injection of AMD3100 after IR injury improves cardiac performance by enhancing the preservation and/or recovery of functional myocardial tissue.

AMD3100 Preferentially Enhances the Mobilization of BM Cells After IR Injury

Because AMD3100 is a CXCR4 antagonist and has been shown to enhance the mobilization of stem/progenitor cells from BM to PB after permanent ligation of the coronary artery,[17] we investigated whether AMD3100 treatment enhanced the mobilization of MNCs, CXCR4$^+$ MNCs, and sca1$^+$/flk1$^+$ MNCs in both uninjured mice and mice with IR injury. PB levels of the 3 types of cells were measured via fluorescence-activated cell sorting, and fluorescence-activated cell sorting measurements of sca1$^+$/flk1$^+$ MNC levels were corroborated via the EPC culture assay. Tie2$^+$ BM progenitor mobilization was also evaluated by monitoring green fluorescent protein (GFP) expression in the BM of wild-type (WT) mice transplanted with BM from Tie2-GFP transgenic mice, which express GFP from the endothelium-specific Tie2 promoter.

In the absence of injury, fluorescence-activated cell sorting analyses indicated that PB levels of MNCs, including sca1$^+$/flk1$^+$ subpopulation, tended to increase (Figure 2A and C) and CXCR4$^+$ MNCs significantly increased after AMD3100 treatment (Figure 2B). The time course of mobilization in the 3 cell types was almost similar: Cell counts tended to peak within 3 hours after AMD3100 administration and returned to near pretreatment levels by 24 hours (Figure 2A–2C). After IR injury, AMD3100 treatment did not alter PB MNC levels (Figure 2D), but PB CXCR4$^+$ MNC counts (Figure 2E) and sca1$^+$/flk1$^+$ MNC counts (Figure 2F) were significantly higher 1 and 3 days, respectively, after injury in AMD3100-treated mice than in mice administered saline. The enhanced mobilization of CXCR4$^+$ MNCs diminished by day 3, whereas PB sca1$^+$/flk1$^+$ MNC counts remained significantly higher in the AMD3100-treated mice than in the saline-treatment group through day 7. When evaluated via culture assay, PB EPC levels (ie, the number of cells stained positively for both lectin and acetylated low-density lipoprotein) were significantly higher in the AMD3100-treated mice than in the saline-treated mice on days 3 and 7 after IR injury (Figure I in the

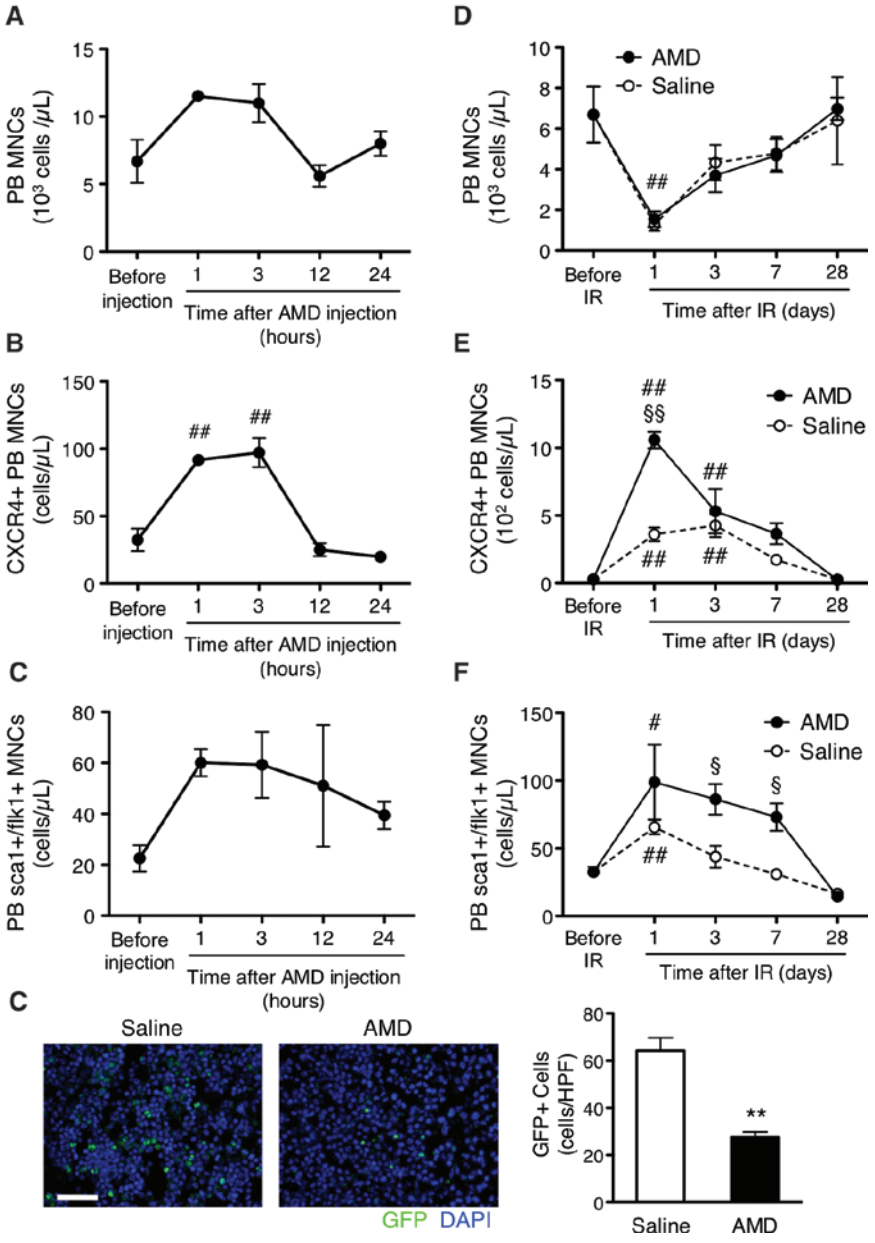

Figure 2. AMD3100 enhances the mobilization of circulating CXC-chemokine receptor 4–positive (CXCR4⁺) mononuclear cells (MNCs) and Sca1⁺/Flk1⁺ cells after ischemia/reperfusion (IR) injury. **A** through **C**, Peripheral blood (PB) levels of (**A**) MNCs, (**B**) CXCR4⁺ MNCs, and (**C**) sca1⁺/flk1⁺ cells were determined in uninjured mice before injection of AMD3100 (125 μg in100 μL saline) and from 1 to 24 hours afterward. **D** through **F**, PB levels of (**D**) MNCs, (**E**) CXCR4⁺ MNCs, and (**F**) sca1⁺/flk1⁺ cells were determined in mice before IR injury and treatment with AMD3100 or saline and from 1 to 28 days afterward. MNC levels were measured with a Hema-Vet hematology system, and the levels of CXCR4⁺ MNCs and sca1⁺/flk1⁺ cells were measured via fluorescence-activated cell sorter analyses of MNCs labeled with fluorescent CXCR4 antibodies (CXCR4⁺ MNCs) or double-labeled with fluorescent Sca1 antibodies and Flk1 antibodies. **G**, IR injury was surgically induced in wild-type mice that had been transplanted with bone marrow (BM) from mice with Tie2-regulated green fluorescent protein (GFP) expression. Mice were treated with AMD3100 or saline after injury, and the number of GFP⁺ BM cells was determined 5 days later. Scale bar=100 μm. **A** through **C**, n=3; **D** through **F**, n=3 to 5 per treatment group at each time point; **G**, n=8 per treatment group. The SEMs are too small to be visible graphically in **A**, hour 1; **B**, hours 1 and 24; **E**, before IR, day 7 (saline), and day 28; and **F**, day 7 (saline) and day 28. #Bonferroni-adjusted $P<0.05$ and ##Bonferroni-adjusted $P<0.01$ vs before injection/IR; §Bonferroni-adjusted $P<0.05$, §§Bonferroni-adjusted $P<0.01$ and $^{**}P<0.01$ vs saline.

online-only Data Supplement), and in mice with Tie2-GFP BM, GFP-expressing cells were significantly less common in BM from the AMD3100-treated group than in BM from saline-treated animals on day 5 after IR injury (Figure 2G). Thus, AMD3100 appears to rapidly but briefly enhance the mobilization of CXCR4⁺ MNCs after IR injury, which is consistent with the role of AMD3100 as a CXCR4 antagonist. However, the effect of AMD3100 on sca1⁺/flk1⁺ MNC mobilization is delayed, more durable, and consequently likely mediated by a different mechanism.

AMD3100 Increases the Contribution of BM-Derived Progenitors to Vascular Growth After IR Injury

To determine whether the enhanced BMPC mobilization observed in mice treated with AMD3100 after IR injury was accompanied by improved vascularity in the AAR, the functional vasculature of injured mice was stained via in vivo perfusion with BS1-lectin before the mice were killed. Experiments were performed in WT mice transplanted with BM from enhanced GFP–expressing mice to enable identification of BM-derived cells in the vasculature. Compared with observations in saline-treated mice, the AAR of AMD3100-treated mice contained significantly more GFP⁺ cells on day 3 after injury (Figure 3A and 2B) and significantly more GFP⁺ cells, GFP-lectin double-positive cells (Figure 3C and 3D), and lectin⁺ vessel density (Figure 3C and 3E) on day 28. AMD3100 treatment also kept elevated SDF-1 expression levels in AAR through day 3 to 7 after IR injury in mice with WT BM (Figure II in the online-only Data Supplement), which likely contributed to the enhanced incorporation of BM-derived cells, perhaps including EPCs.

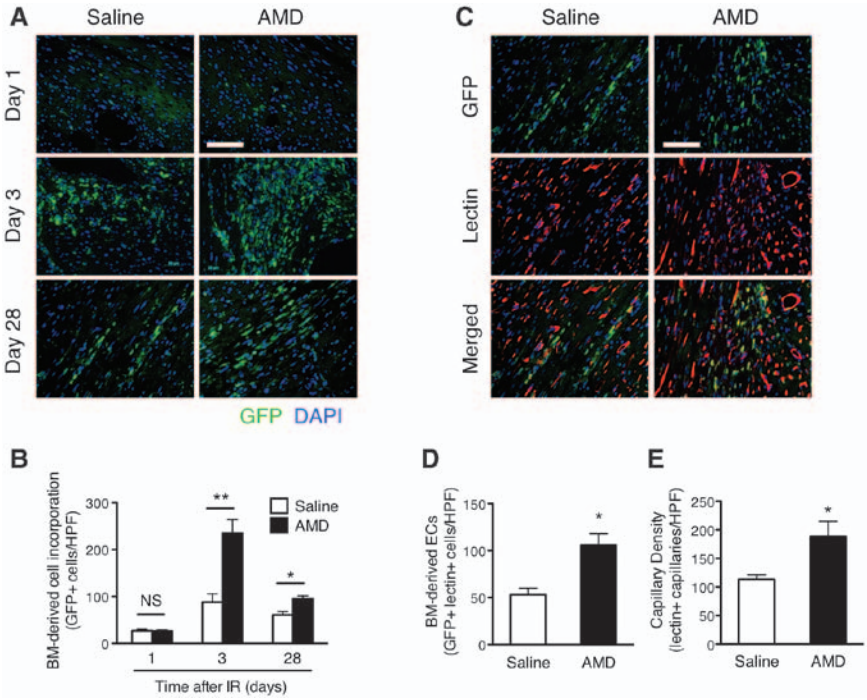

Figure 3. AMD3100 increases capillary density and the number of bone marrow (BM)–derived endothelial cells in the myocardium after ischemia/reperfusion (IR) injury. AMD3100 or saline was subcutaneously injected after IR injury in wild-type mice that had been transplanted with BM from green fluorescent protein (GFP)–expressing mice. **A** and **B**, BM-derived (ie, GFP-expressing) cells (green) were identified in the area at risk (AAR) and quantified on days 1, 3, and 28 after injury. Scale bar=100 μm. **C** through **E**, On day 28 after IR injury, mice were perfused with BS1-lectin before death, and sections from the AAR were stained with fluorescent anti-lectin antibodies. **C**, BM-derived endothelial cells (ECs) were quantified as the number of cells positive for both GFP expression and lectin staining. Scale bar=100 μm. **D**, BM-derived cells (green, GFP fluorescence) and functional vascular structures (red, lectin fluorescence) were identified in the AAR, and (**E**) capillary density was quantified as the number of lectin$^+$ vascular structures. **B**, n=3 to 6 per treatment group at each time point; **D** and **E**, n=3 to 4 per treatment group. *P<0.05 and **P<0.01 vs saline.

AMD3100 Increases BM Endothelial Nitric Oxide Synthase Expression and the Number of Endothelial Nitric Oxide Synthase–Expressing BM-Derived Cells in the AAR After IR Injury

Endothelial nitric oxide synthase (eNOS) is a key regulator of endothelial cell growth and migration, vascular remodeling, and angiogenesis[21–23] and has recently been shown to have an important role in the activity of stem and progenitor cells. We investigated whether the enhanced functional recovery and BMPC mobilization associated with AMD3100 administration after IR injury are accompanied by increases in eNOS activity.

From day 1 through day 7 after IR injury, eNOS-expressing cells were significantly more common in the BM of AMD3100-treated mice than in the BM of mice administered saline (Figure 4A). AMD3100 treatment was also associated with higher BM protein levels of matrix metalloproteinase-9 and soluble Kit ligand,[24] 2 downstream components of the eNOS pathway, from day 1 and 3, respectively, through day 7 (Figure 4B and 4C) and with higher PB levels of nitrate and nitrite (ie, the final metabolites of nitric oxide) on day 3 (Figure 4D). In mice transplanted with BM from transgenic GFP-expressing mice, the number of cells in the AAR that expressed eNOS, GFP, or both eNOS and GFP was significantly higher in AMD3100-treated mice than in saline-treated mice on day 3 after injury (Figure 4E–4H). Thus, AMD3100 administration after IR injury appears to increase eNOS activity in both the BM and the ischemic region.

The direct influence of AMD3100 on eNOS activity was investigated by determining whether AMD3100 treatment altered eNOS mRNA expression and nitrate/nitrite production in cultured BMPCs or luciferase activity in murine endothelial cells transfected with a gene coding for luciferase expression from the eNOS promoter. AMD3100 treatment was associated with higher levels of both eNOS expression and nitrate/nitrite production in BMPCs (Figure IIIA and IIIB in the online-only Data Supplement), and AMD3100 dose-dependently increased luciferase activity in transfected endothelial cells (Figure IIIC in the online-only Data Supplement). Collectively, these observations suggest that the benefits associated with AMD3100 administration are accompanied by increases in eNOS activity.

The Benefit of AMD3100 Treatment After IR Injury Is Dependent on eNOS Expression in the BM but Not in the Ischemic Region

To determine whether eNOS expression contributes to the benefits associated with AMD3100 administration after IR injury and, if so, whether that contribution comes from BM cells or from cells already present in the ischemic tissue, we evaluated the influence of AMD3100 on myocardial recovery in eNOS-knockout mice that had been transplanted with BM from WT mice (eNOS-KO/WT_{BM}) and in WT mice transplanted with BM from eNOS-KO mice (WT/eNOS-KO_{BM}). An identical set of assessments was performed in WT mice transplanted with WT BM (WT/WT_{BM}).

In eNOS-KO/WT_{BM} mice, LV fractional shortening on days 14 and 28 after IR injury was significantly greater with AMD3100 treatment than with saline treatment, but the functional benefit of AMD3100 treatment was not observed in WT/eNOS-KO_{BM} mice at any time point (Figure 5A and 5B and Table II in the online-only Data Supplement). Similarly, AMD3100 treatment in eNOS-KO/WT_{BM} mice but not in WT/eNOS-KO_{BM} mice was associated with greater numbers of eNOS$^+$ BM cells, elevated BM matrix metalloproteinase-9 and soluble Kit ligand protein expression, higher PB sca1$^+$/flk1$^+$ MNC counts, less cardiac apoptosis, and smaller infarcts on day 3 after injury (Figure 5D–5I) and with less cardiac

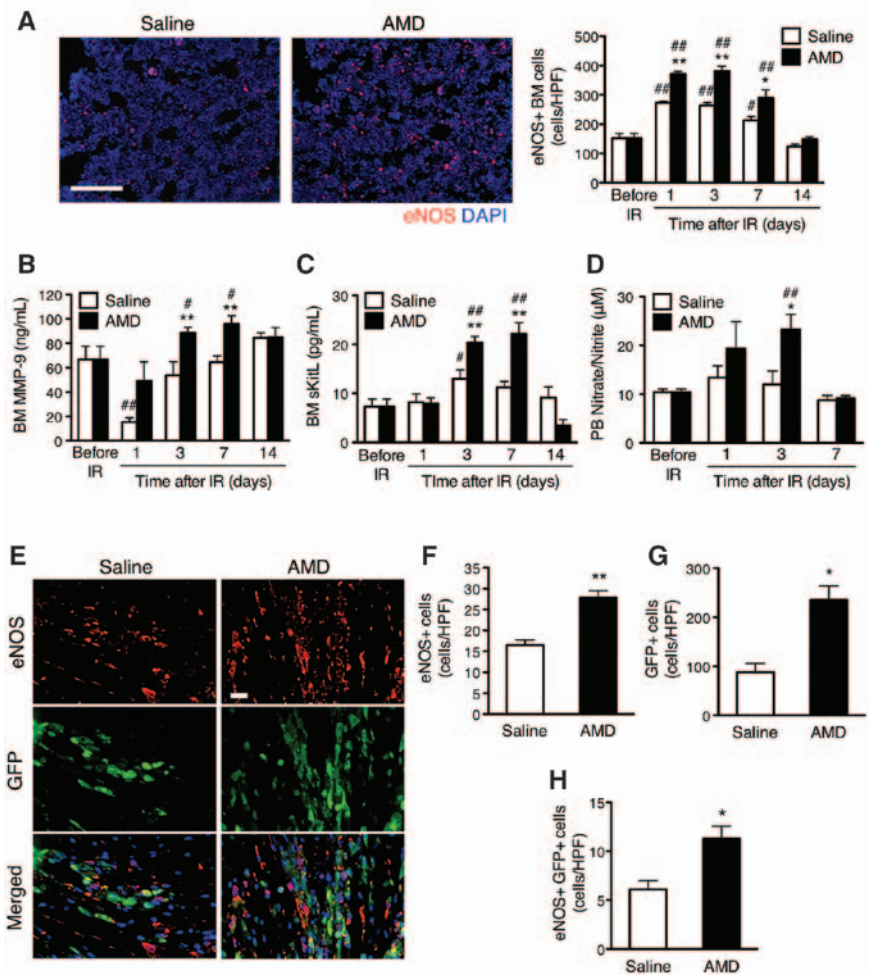

Figure 4. AMD3100 increases bone marrow (BM) endothelial nitric oxide synthase (eNOS) expression and the number of eNOS-expressing BM-derived cells in the area at risk (AAR) after ischemia/reperfusion (IR) injury. AMD3100 or saline was subcutaneously injected after IR injury in (**A**–**D**) wild-type (WT) mice and (**E**–**H**) WT mice that had been transplanted with BM from green fluorescent protein (GFP)–expressing mice. **A** through **C**, BM was harvested from mice euthanized before IR injury and from 1 to 14 days afterward. **A**, BM cells were labeled with fluorescent anti-eNOS antibodies (red), and eNOS$^+$ cells were quantified. Scale bar=100 μm. **B** and **C**, BM plasma levels of (**B**) matrix metalloproteinase-9 (MMP-9) and (**C**) soluble Kit ligand (sKitL) protein were determined via ELISA. **D**, Peripheral blood (PB) levels of nitrate and nitrite were determined via colorimetric assay before IR injury and 1 to 14 days afterward. **E**, eNOS (red) and GFP (green) expression was evaluated in sections from the AAR of mice euthanized 3 days after IR injury. Scale bar=20 μm. Cells positive for the expression of (**F**) eNOS, (**G**) GFP, or (**H**) both eNOS and GFP were quantified. **A** through **D**, n=4 to 8 per treatment group at each time point; **F** through **H**, n=3 to 5 per treatment group. HPF indicates high-power field. #*P*<0.05 and ##*P*<0.01 vs before injection; **P*<0.05 and ***P*<0.01 vs saline.

fibrosis and greater capillary density on day 28 (Figure 5J and 5K). The results associated with AMD3100 treatment in WT/WT$_{BM}$ mice matched those observed in eNOS-KO/WT$_{BM}$ mice (Figure 5C–5K), and the only treatment-related effect observed in all 3 chimeric mouse lines was the enhanced mobilization of CXCR4$^+$ MNCs, which occurred on day 1 after injury and diminished by day 3 (Figure 5L). Thus, the benefits associated with AMD3100 administration after IR injury require eNOS expression in the BM but not in the ischemic region, and eNOS appears to have a role in the mobilization of sca1$^+$/flk1$^+$ MNCs but not CXCR4$^+$ MNCs.

The Expression of eNOS by PB EPCs Contributes to Myocardial Recovery but Is Not Required for EPC Incorporation

Because BM eNOS expression is required for both the beneficial effects of AMD3100 treatment after IR injury and the mobilization of progenitors from BM to PB, we investigated whether eNOS expression in circulating BMPCs contributes to myocardial recovery. BMPCs were isolated from WT mice and eNOS-KO mice, cultured for 4 days, and then intravenously injected into WT mice 24 hours after IR injury; a third group of mice were injected with saline. Fourteen and 28 days after IR injury, LV fractional shortening was significantly greater in mice administered WT BMPCs than in mice administered saline, but the difference between treatment with eNOS-KO BMPCs and saline administration did not reach statistical significance (Figure 6A and Table II in the online-only Data Supplement).

To determine whether the expression of eNOS by circulating BMPCs contributes to myocardial recovery by increasing the incorporation and whether AMD3100 enhances the incorporation of circulating BMPCs, WT and eNOS-KO EPCs were labeled with DiI and intravenously injected into WT mice 24 hours after IR injury and treatment with AMD3100 or saline. Mice were euthanized 3 days after IR injury for histological analyses. Neither the type of cell injected (ie, eNOS-KO or WT) nor the treatment administered (ie, AMD3100 or saline) significantly influenced the incorporation of injected cells (Figure 6B). Nevertheless, apoptotic cells were significantly less common and infarct sizes were significantly smaller in mice administered WT BMPCs than in mice administered eNOS-KO BMPCs, regardless of treatment group, and measurements in mice administered eNOS-KO BMPCs did not differ significantly from those in saline-treated mice (Figure 6C and 6D).

Collectively, these observations suggest that the expression of eNOS by circulating BMPCs does not have a role in their recruitment and incorporation but does contribute to cardiac protection. Therefore, the greater number of BM-derived endothelial cells observed in the AAR of AMD3100-treated mice (Figure 3C) appears to evolve primarily through

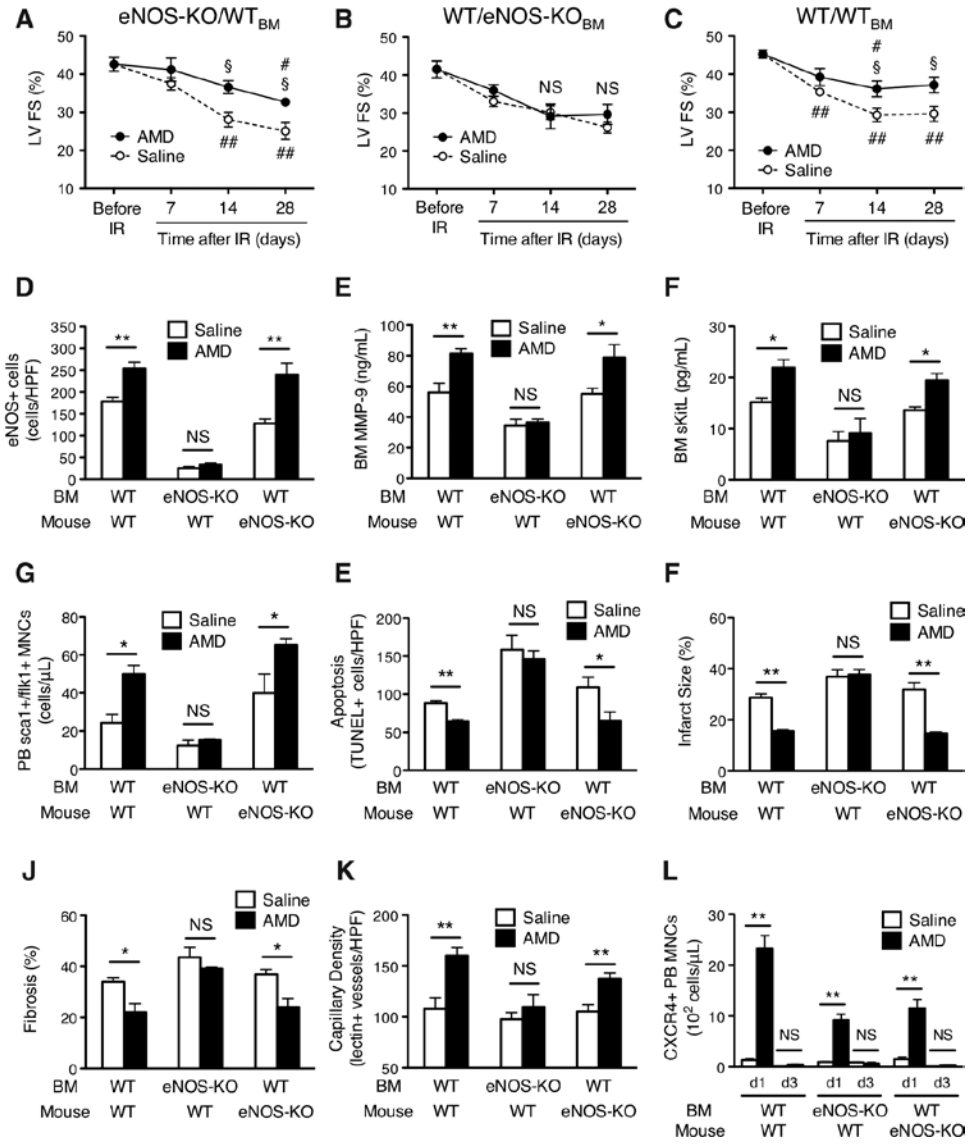

Figure 5. The benefit of AMD3100 treatment after ischemia/reperfusion (IR) injury is dependent on endothelial nitric oxide synthase (eNOS) expression in the bone marrow (BM) but not in the ischemic tissue. AMD3100 or saline was subcutaneously injected after IR injury in eNOS-knockout mice that had been transplanted with BM from wild-type (WT) mice (eNOS-KO/WT$_{BM}$), in WT mice transplanted with BM from eNOS-KO mice (WT/eNOS-KO$_{BM}$), and in WT mice transplanted with WT BM (WT/WT$_{BM}$). **A** through **C**, Echocardiographic assessments of left ventricular fractional shortening (LV FS) were performed before IR injury and 7 to 28 days afterward. **D** through **F**, BM was harvested 3 days after IR injury. **D**, BM cells were labeled with fluorescent anti-eNOS antibodies, and positively stained cells were quantified. **E** and **F**, BM plasma levels of (**E**) matrix metalloproteinase-9 (MMP-9) and (**F**) soluble Kit ligand (sKitL) protein were determined via ELISA. **G**, Three days after IR injury, mononuclear cells (MNCs) were isolated from the peripheral blood (PB) and labeled with fluorescent anti-Sca1 and anti-Flk1 antibodies, and the number of MNCs positive for both Sca1 and Flk1 expression was determined via fluorescence-activated cell sorting (FACS) analysis. **H**, Sections from the area at risk (AAR) of mice euthanized on day 3 after IR injury were stained with terminal deoxynucleotidyl transferase dUTP nick-end labeling (TUNEL), and apoptosis was quantified as the number of positively stained cells. **I**, Infarct size and AAR were assessed via in vivo microsphere perfusion and triphenyltetrazolium chloride staining in mice euthanized on day 3 after IR injury; the ratio of the area of the infarct to the AAR was presented as a percentage. **J**, Fibrosis on day 28 after IR injury was assessed in Masson trichrome–stained heart sections, quantified as the ratio of the length of fibrosis to the left ventricular circumference, and presented as a percentage. **K**, Capillary density was assessed in mice that had been perfused with BS1-lectin before death on day 28 after IR injury and quantified as the number of lectin$^+$ vascular structures. **L**, MNCs were harvested from the PB on day 1 (d1) and day 3 (d3) after IR injury and labeled with fluorescent anti-CXCR4 antibodies, and the number of CXCR4$^+$ MNCs was determined via FACS. **A** through **C**, n=4 to 8 per treatment group at each time point; **D**, n=3 to 4 per treatment group; **E**, n=4 to 8 per treatment group; **F**, n=5 to 9 per treatment group; **G** through **J**, n=3 to 6 per treatment group; **K**, n=3 per treatment group; **L**, n=3 to 6 per treatment group at each time point. The SEM is too small to be visible graphically for **C**, day 7 (saline). HPF indicates high-power field. ##Bonferroni-adjusted $P<0.01$ vs before injection; §Bonferroni-adjusted $P<0.05$, $^*P<0.05$, and $^{**}P<0.01$ vs saline.

enhanced BMPC mobilization, which subsequently increases the number of the progenitors available in the circulation, rather than by directly influencing the recruitment and incorporation of circulating cells.

Discussion

In the present study, we have shown that AMD3100, a CXCR4 antagonist, had a beneficial effect on cardiac IR injury that closely mimics coronary intervention in acute myocardial

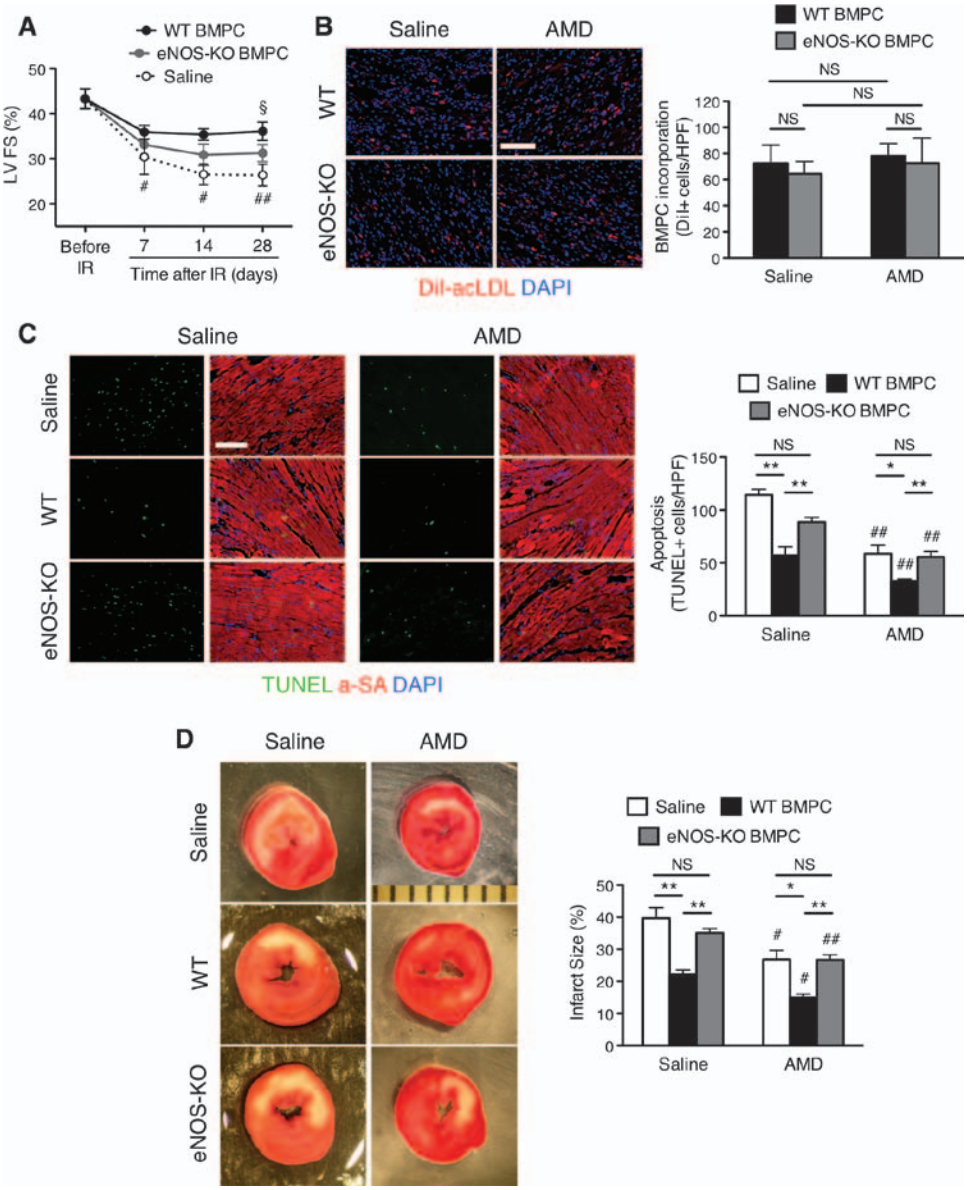

Figure 6. The expression of endothelial nitric oxide synthase (eNOS) by circulating bone marrow progenitor cells (BMPCs) contributes to myocardial recovery. **A**, BMPCs from wild-type (WT) mice, BMPCs from eNOS-knockout (KO) mice, or saline was intravenously injected into WT mice 24 hours after ischemia/reperfusion (IR) injury. Echocardiographic assessments of left ventricular fractional shortening (LV FS) were performed before IR injury and 7 to 28 days afterward. **B** through **D**, DiI-labeled WT BMPCs, DiI-labeled eNOS-KO BMPCs, or saline was intravenously injected into WT mice 24 hours after IR injury, along with treatment with subcutaneous injections of AMD3100 or saline. Mice were euthanized 2 days later (ie, 3 days after IR injury). §Bonferroni-adjusted $P<0.05$ vs saline; #$P<0.05$ and ##$P<0.01$ vs before injection. **B**, Incorporation of the injected cells was evaluated by quantifying the number of DiI-positive cells in the area at risk (AAR). Scale bar=100 μm. **C**, Sections from the AAR were stained with terminal deoxynucleotidyl transferase dUTP nick-end labeling (TUNEL; green), stained with fluorescent anti–α-sarcomeric actin (a-SA) antibodies (red), and counterstained with DAPI (blue). Scale bar=100 μm. Apoptosis was quantified as the number of TUNEL⁺ cells. **D**, Infarct size and AAR were assessed via in vivo microsphere perfusion and triphenyltetrazolium chloride staining; viable tissue appears deep red and the infarcted region is colorless. The ratio of the area of the infarct to the AAR was presented as a percentage. *$P<0.05$ and **$P<0.01$, #$P<0.05$ and ##$P<0.01$ vs the same intravenous injection (ie, saline, WT BMPCs, or eNOS-KO BMPCs) in animals treated with subcutaneous injections of saline. **A**, n=4 to 5 per treatment group at each time point; **B**, n=3 to 5 per group; **C**, n=3 to 7 per group; **D**, n=4 to 7 per group. acLDL indicates acetylated low-density lipoprotein; and HPF, high-power field.

infarction patients. AMD3100 enhanced the mobilization of BM-derived progenitor cells, including EPCs, that were incorporated into AAR and exerted cardioprotective effects by antiapoptosis and anti-inflammation in the acute phase and revascularizing effects in the remote phase, resulting in minimization of scar size and preservation of cardiac functions.

AMD3100 has been approved by the US Food and Drug Administration for use as a stem cell mobilizing agent[25]; however, few reports have evaluated the time course and subpopulations of cells mobilized by AMD3100 administration after IR injury. Our results indicate that rapid accumulation of circulating MNCs, specifically inflammatory cells, into AAR accounts for the decreased number of MNCs in PB on day 1

after IR injury. On the other hand, IR injury could be a trigger to mobilize progenitors (ie, CXCR4$^+$ or sca-1$^+$/flk1$^+$ MNCs, including EPCs) from BM, resulting in the increased number of progenitors in PB. AMD3100 increased the mobilization of CXCR4$^+$ cells on day 1 after IR injury by disrupting SDF-1–CXCR4 binding in BM, but this enhancement dissipated before the expression of SDF-1, a ligand of CXCR4, was upregulated in ischemic myocardium on day 3 after IR injury. The delay in SDF-1 upregulation may explain why the rapid mobilization of CXCR4$^+$ cells did not result in a dramatic increase in BM-derived cell recruitment to the AAR on day 1 after IR injury. The AMD3100-induced delayed enhancement of sca1$^+$/flk1$^+$ MNC mobilization coincided with elevated BM levels of eNOS and 2 eNOS-targeted proteins, matrix metalloproteinase-9 and soluble Kit ligand, that have been linked to progenitor cell mobilization,[24,26] and the enhanced mobilization of progenitors required BM eNOS expression.

eNOS is known to protect cardiomyocytes against apoptosis,[27,28] and AMD3100 treatment led to increases in the number of eNOS-expressing cells, to declines in the number of apoptotic cells, and to a reduction in infarct sizes in AAR on day 3 after IR injury. Similarly, systemically injected eNOS-expressing WT BMPCs but not eNOS-KO BMPCs were associated with less apoptosis and smaller infarct sizes in both AMD3100-treated and saline-treated mice on day 3 after injury, even though the number of recruited cells in both cell types in the AAR was similar. Additionally, in IR-injured mice without AMD3100 treatment, eNOS expression in BM was upregulated by myocardial transient ischemia alone from day 1 through 7; therefore, AMD3100 was assumed to give an extra elevation of eNOS production in BM cells over ischemic insult.

In the mechanistic aspect, it was reported that eNOS-expressing cells enhanced vascular endothelial growth factor (VEGF) protein production.[29] As known broadly, VEGF upregulates eNOS expression, suggesting that initial upregulation of eNOS expression was sustained up to day 7 after IR injury with AMD3100 treatment via an autocrine mechanism involving the VEGF-eNOS signaling pathway. We previously showed that VEGF played a crucial role in mobilizing progenitors from BM into PB in a mouse coronary ligation model. However, in the present study, we confirmed a direct effect of AMD3100 on eNOS upregulation by reporter assay (Figure IIIC in the online-only Data Supplement). In addition, eNOS mRNA expression was upregulated >2-fold in the AMD3100-treated BMPCs compared with control BM PCs, whereas VEGF mRNA expression was limited to a <2-fold increase in the AMD3100-treated group (Figure IV in the online-only Data Supplement). Thus, AMD3100 could directly enhance eNOS production in the recruited cultured BMPCs in ischemic myocardium, suggesting that AMD3100 might exhibit a cardioprotective effect via the recruited BMPC-derived eNOS production, at least in part, in the WT and eNOS-KO BMPC injection experiment. In addition, on the basis of the evidence that eNOS promoted angiogenesis and reduced apoptosis by inhibition of transforming growth factor-β1 signaling,[30] imported BMPC-derived eNOS may contribute to enhance capillary density after IR injury via a similar mechanism. Thus, the cardioprotective effects of AMD3100-induced eNOS activity are a crucial component of the response to IR injury, but these effects appear to evolve primarily from BM-derived progenitors rather than from cells already present in the AAR.

In terms of the contribution of the mobilized BM-derived progenitors by AMD3100 to ischemic myocardium, although there is no direct evidence that circulating CXCR4$^+$ cells incorporated into the AAR in the acute phase after IR, the peak number of mobilized CXCR4$^+$ cells was striking (10 times more than that of mobilized sca1$^+$/flk1$^+$ cells); therefore, CXCR4$^+$ cells may play a role in the AAR. Referring to the reports in which CXCR4-expressing cells were shown to enhance incorporation into ischemic area and to improve cardiac function after myocardial infarction[31,32] and the fact that the plasma half-life of AMD3100 is very short (3.5 hours) in circulation, mobilized CXCR4$^+$ cells might not be affected by its recruitment to SDF-1–releasing sites of ischemia at day 1 to 3 after IR injury. Even though the eNOS KO- or WT-cultured BMPC infusion study did not show significant differences in cultured BMPC recruitment to sites of ischemia, endogenous progenitors, namely CXCR4$^+$ cells and sca1$^+$/flk1$^+$ cells mobilized by AMD3100, might recruit to ischemic myocardium, exhibiting cardioprotective effects, because SDF-1 and VEGF are released from ischemic myocardium and recruit circulating progenitors expressing receptors of CXCR4[31] and flk1.[33]

The findings presented here indicate that AMD3100 improves the recovery of cardiac function after IR injury and that the beneficial effect of AMD3100 on ischemic heart with IR injury requires eNOS expression in BM but not in myocardium. AMD3100 sustains the mobilization of sca1$^+$/flk1$^+$ MNCs rather than CXCR4$^+$ MNCs, resulting in the increased number of recruited BM-derived eNOS-expressing cells, and contributes to limiting infarct size, reducing cardiac apoptosis, and increasing vascularity in ischemic myocardium. Collectively, single treatment with AMD3100 may give rise to a novel supportive therapy in percutaneous transluminal coronary angioplasty and stenting for acute coronary syndrome via a cardioprotection/proangiogenesis-dependent mechanism.

Study Limitations

In this study, we have not definitively identified the mobilized BM-derived cells by AMD3100, including sca1$^+$/flk1$^+$ MNCs and CXCR4$^+$ cells, providing direct evidence for the incorporation into vascular structure, however, we and others have previously demonstrated that not the majority but a certain extent of these BM-derived cells were exactly incorporated into neovasculature in ischemic tissue.[31,32,34–36] In addition, because we have focused on the therapeutic effect of AMD3100 with its eNOS-dependent BMPC mobilization in PB and the recruitment to sites of IR injury, we have not tried to identify what type of cells, so-called EPCs, defined by multiple cell surface markers are incorporated into the neovasculature. The precise definition of human/mouse EPCs remains unclear and would be quite difficult to ascertain.

Acknowledgments

We thank Kari Krueger for administrative assistance and W. Kevin Meisner, PhD, ELS, for editorial support. The work presented in this article was performed at the Feinberg Cardiovascular Research

Institute, Northwestern University Feinberg School of Medicine, Chicago, IL.

Sources of Funding

This work was supported in part by the US National Institutes of Health (grants HL053354-14, HL057516-12, HL080137-05, HL095874-04, HL093439-03, and HL113541-01).

Disclosures

Dr Losordo is an employee of Baxter Healthcare. The other authors report no conflicts.

References

1. Murasawa S, Kawamoto A, Horii M, Nakamori S, Asahara T. Niche-dependent translineage commitment of endothelial progenitor cells, not cell fusion in general, into myocardial lineage cells. *Arterioscler Thromb Vasc Biol*. 2005;25:1388–1394.
2. Shintani S, Murohara T, Ikeda H, Ueno T, Honma T, Katoh A, Sasaki K, Shimada T, Oike Y, Imaizumi T. Mobilization of endothelial progenitor cells in patients with acute myocardial infarction. *Circulation*. 2001;103:2776–2779.
3. Brenner W, Aicher A, Eckey T, Massoudi S, Zuhayra M, Koehl U, Heeschen C, Kampen WU, Zeiher AM, Dimmeler S, Henze E. 111In-labeled CD34+ hematopoietic progenitor cells in a rat myocardial infarction model. *J Nucl Med*. 2004;45:512–518.
4. Mohle R, Bautz F, Rafii S, Moore MA, Brugger W, Kanz L. The chemokine receptor CXCR-4 is expressed on CD34+ hematopoietic progenitors and leukemic cells and mediates transendothelial migration induced by stromal cell-derived factor-1. *Blood*. 1998;91:4523–4530.
5. Peled A, Grabovsky V, Habler L, Sandbank J, Arenzana-Seisdedos F, Petit I, Ben-Hur H, Lapidot T, Alon R. The chemokine SDF-1 stimulates integrin-mediated arrest of CD34(+) cells on vascular endothelium under shear flow. *J Clin Invest*. 1999;104:1199–1211.
6. Yamaguchi J, Kusano KF, Masuo O, Kawamoto A, Silver M, Murasawa S, Bosch-Marce M, Masuda H, Losordo DW, Isner JM, Asahara T. Stromal cell-derived factor-1 effects on ex vivo expanded endothelial progenitor cell recruitment for ischemic neovascularization. *Circulation*. 2003;107:1322–1328.
7. Aiuti A, Webb IJ, Bleul C, Springer T, Gutierrez-Ramos JC. The chemokine SDF-1 is a chemoattractant for human CD34+ hematopoietic progenitor cells and provides a new mechanism to explain the mobilization of CD34+ progenitors to peripheral blood. *J Exp Med*. 1997;185:111–120.
8. Wang JF, Liu ZY, Groopman JE. The alpha-chemokine receptor CXCR4 is expressed on the megakaryocytic lineage from progenitor to platelets and modulates migration and adhesion. *Blood*. 1998;92:756–764.
9. Lataillade JJ, Clay D, Dupuy C, Rigal S, Jasmin C, Bourin P, Le Bousse-Kerdiles MC. Chemokine SDF-1 enhances circulating CD34(+) cell proliferation in synergy with cytokines: possible role in progenitor survival. *Blood*. 2000;95:756–768.
10. Este JA, Cabrera C, De Clercq E, Struyf S, Van Damme J, Bridger G, Skerlj RT, Abrams MJ, Henson G, Gutierrez A, Clotet B, Schols D. Activity of different bicyclam derivatives against human immunodeficiency virus depends on their interaction with the CXCR4 chemokine receptor. *Mol Pharmacol*. 1999;55:67–73.
11. Gerlach LO, Skerlj RT, Bridger GJ, Schwartz TW. Molecular interactions of cyclam and bicyclam non-peptide antagonists with the CXCR4 chemokine receptor. *J Biol Chem*. 2001;276:14153–14160.
12. Hatse S, Princen K, Bridger G, De Clercq E, Schols D. Chemokine receptor inhibition by AMD3100 is strictly confined to CXCR4. *FEBS Lett*. 2002;527:255–262.
13. Hendrix CW, Flexner C, MacFarland RT, Giandomenico C, Fuchs EJ, Redpath E, Bridger G, Henson GW. Pharmacokinetics and safety of AMD-3100, a novel antagonist of the CXCR-4 chemokine receptor, in human volunteers. *Antimicrob Agents Chemother*. 2000;44:1667–1673.
14. Broxmeyer HE, Orschell CM, Clapp DW, Hangoc G, Cooper S, Plett PA, Liles WC, Li X, Graham-Evans B, Campbell TB, Calandra G, Bridger G, Dale DC, Srour EF. Rapid mobilization of murine and human hematopoietic stem and progenitor cells with AMD3100, a CXCR4 antagonist. *J Exp Med*. 2005;201:1307–1318.
15. Liles WC, Broxmeyer HE, Rodger E, Wood B, Hubel K, Cooper S, Hangoc G, Bridger GJ, Henson GW, Calandra G, Dale DC. Mobilization of hematopoietic progenitor cells in healthy volunteers by AMD3100, a CXCR4 antagonist. *Blood*. 2003;102:2728–2730.
16. Devine SM, Flomenberg N, Vesole DH, Liesveld J, Weisdorf D, Badel K, Calandra G, DiPersio JF. Rapid mobilization of CD34+ cells following administration of the CXCR4 antagonist AMD3100 to patients with multiple myeloma and non-Hodgkin's lymphoma. *J Clin Oncol*. 2004;22:1095–1102.
17. Jujo K, Hamada H, Iwakura A, Thorne T, Sekiguchi H, Clarke T, Ito A, Misener S, Tanaka T, Klyachko E, Kobayashi K, Tongers J, Roncalli J, Tsurumi Y, Hagiwara N, Losordo DW. CXCR4 blockade augments bone marrow progenitor cell recruitment to the neovasculature and reduces mortality after myocardial infarction. *Proc Natl Acad Sci USA*. 2010;107:11008–11013.
18. Asahara T, Masuda H, Takahashi T, Kalka C, Pastore C, Silver M, Kearne M, Magner M, Isner JM. Bone marrow origin of endothelial progenitor cells responsible for postnatal vasculogenesis in physiological and pathological neovascularization. *Circ Res*. 1999;85:221–228.
19. Asahara T, Takahashi T, Masuda H, Kalka C, Chen D, Iwaguro H, Inai Y, Silver M, Isner JM. VEGF contributes to postnatal neovascularization by mobilizing bone marrow-derived endothelial progenitor cells. *EMBO J*. 1999;18:3964–3972.
20. Ii M, Nishimura H, Iwakura A, Wecker A, Eaton E, Asahara T, Losordo DW. Endothelial progenitor cells are rapidly recruited to myocardium and mediate protective effect of ischemic preconditioning via "imported" nitric oxide synthase activity. *Circulation*. 2005;111:1114–1120.
21. Pipili-Synetos E, Sakkoula E, Maragoudakis ME. Nitric oxide is involved in the regulation of angiogenesis. *Br J Pharmacol*. 1993;108:855–857.
22. Ziche M, Morbidelli L, Masini E, Granger HJ, Gepetti P, Ledda F. Nitric oxide promotes DNA synthesis and cyclic GMP formation in endothelial cells from post capillary venules. *Biochem Biophys Res Commun*. 1993;192:1198–1203.
23. Ziche M, Morbidelli L, Masini E, Amerini S, Granger HJ, Maggi CA, Geppetti P, Ledda F. Nitric oxide mediates angiogenesis *in vivo* and endothelial cell growth and migration *in vitro* promoted by substance P. *J Clin Invest*. 1994;94:2036–2044.
24. Aicher A, Heeschen C, Mildner-Rihm C, Urbich C, Ihling C, Technau-Ihling K, Zeiher AM, Dimmeler S. Essential role of endothelial nitric oxide synthase for mobilization of stem and progenitor cells. *Nat Med*. 2003;9:1370–1376.
25. Steinberg M, Silva M. Plerixafor: a chemokine receptor-4 antagonist for mobilization of hematopoietic stem cells for transplantation after high-dose chemotherapy for non-Hodgkin's lymphoma or multiple myeloma. *Clin Ther*. 2010;32:821–843.
26. Heissig B, Hattori K, Dias S, Friedrich M, Ferris B, Hackett NR, Crystal RG, Besmer P, Lyden D, Moore MA, Werb Z, Rafii S. Recruitment of stem and progenitor cells from the bone marrow niche requires MMP-9 mediated release of Kit-ligand. *Cell*. 2002;109:625–637.
27. Jones SP, Girod WG, Palazzo AJ, Granger DN, Grisham MB, Jourd'Heuil D, Huang PL, Lefer DJ. Myocardial ischemia-reperfusion injury is exacerbated in absence of endothelial cell nitric oxide synthase. *Am J Physiol*. 1999;276:H1567–H1573.
28. Razavi HM, Hamilton JA, Feng Q. Modulation of apoptosis by nitric oxide: implications in myocardial ischemia and heart failure. *Pharmacol Ther*. 2005;106:147–162.
29. Mees B, Recalde A, Loinard C, Tempel D, Godinho M, Vilar J, van Haperen R, Levy B, de Crom R, Silvestre JS. Endothelial nitric oxide synthase overexpression restores the efficiency of bone marrow mononuclear cell-based therapy. *Am J Pathol*. 2011;178:55–60.
30. Chen LL, Yin H, Huang J. Inhibition of TGF-beta1 signaling by eNOS gene transfer improves ventricular remodeling after myocardial infarction through angiogenesis and reduction of apoptosis. *Cardiovasc Pathol*. 2007;16:221–230.
31. Zhang D, Fan GC, Zhou X, Zhao T, Pasha Z, Xu M, Zhu Y, Ashraf M, Wang Y. Over-expression of CXCR4 on mesenchymal stem cells augments myoangiogenesis in the infarcted myocardium. *J Mol Cell Cardiol*. 2008;44:281–292.
32. Morimoto H, Takahashi M, Shiba Y, Izawa A, Ise H, Hongo M, Hatake K, Motoyoshi K, Ikeda U. Bone marrow-derived CXCR4+ cells mobilized by macrophage colony-stimulating factor participate in the reduction of infarct area and improvement of cardiac remodeling after myocardial infarction in mice. *Am J Pathol*. 2007;171:755–766.
33. Li J, Brown LF, Hibberd MG, Grossman JD, Morgan JP, Simons M. VEGF, flk-1, and flt-1 expression in a rat myocardial infarction model of angiogenesis. *Am J Physiol*. 1996;270:H1803–1811.

34. Cho HJ, Lee N, Lee JY, Choi YJ, Ii M, Wecker A, Jeong JO, Curry C, Qin G, Yoon YS. Role of host tissues for sustained humoral effects after endothelial progenitor cell transplantation into the ischemic heart. *J Exp Med*. 2007;204:3257–3269.
35. Kawamoto A, Gwon HC, Iwaguro H, Yamaguchi JI, Uchida S, Masuda H, Silver M, Ma H, Kearney M, Isner JM, Asahara T. Therapeutic potential of ex vivo expanded endothelial progenitor cells for myocardial ischemia. *Circulation*. 2001;103:634–637.
36. Chavakis E, Aicher A, Heeschen C, Sasaki K, Kaiser R, El Makhfi N, Urbich C, Peters T, Scharffetter-Kochanek K, Zeiher AM, Chavakis T, Dimmeler S. Role of beta2-integrins for homing and neovascularization capacity of endothelial progenitor cells. *J Exp Med*. 2005;201:63–72.

CLINICAL PERSPECTIVE

Numerous clinical trials with cell therapy focusing on cardiac functional recovery after cardiovascular diseases, including myocardial infarction, have been performed over the past decade. Despite a certain extent of favorable outcome by the evolutional compared with conventional therapies, the trials have been required to overcome ethical, technical, and medical expense issues that may hinder the development of a novel therapeutic strategy. We have shown here that single administration of the CXC-chemokine receptor 4 antagonist AMD3100 exhibited sufficient therapeutic effect on cardiac functional recovery via mobilizing bone marrow–derived endogenous progenitor cells, including endothelial progenitor cells, by an endothelial nitric oxide synthase–dependent mechanism in a mouse ischemia/reperfusion injury model. The easy-to-handle, low-invasiveness, and inexpensive therapy with AMD3100 that we proposed in the present study can avoid the above-described hurdles to be cleared in clinical trials for cell therapy. AMD3100 treatment may not be able to restore cardiac function after myocardial infarction completely but could be a potent supplemental option after the established coronary recanalization/reperfusion technique with percutaneous transluminal coronary angioplasty balloons and stents. Clinical trials of autologous stem/progenitor cell therapy are ongoing, and positive outcomes have emerged, specifically in nonoption patients suffering from severe cardiovascular disease. Our data suggest that AMD3100, an endogenous stem/progenitor cell mobilizer, has the potential to be a simple but promising additional therapy, taking the place of stem/progenitor cell transplantation therapy for ischemic heart diseases.

CXC-Chemokine Receptor 4 Antagonist AMD3100 Promotes Cardiac Functional Recovery After Ischemia/Reperfusion Injury via Endothelial Nitric Oxide Synthase–Dependent Mechanism

Kentaro Jujo, Masaaki Ii, Haruki Sekiguchi, Ekaterina Klyachko, Sol Misener, Toshikazu Tanaka, Jörn Tongers, Jérôme Roncalli, Marie-Ange Renault, Tina Thorne, Aiko Ito, Trevor Clarke, Christine Kamide, Yukio Tsurumi, Nobuhisa Hagiwara, Gangjian Qin, Michio Asahi and Douglas W. Losordo

Circulation. 2013;127:63-73; originally published online November 30, 2012;
doi: 10.1161/CIRCULATIONAHA.112.099242
Circulation is published by the American Heart Association, 7272 Greenville Avenue, Dallas, TX 75231

Print ISSN: 0009-7322. Online ISSN: 1524-4539

Supplemental Material

SUPPLEMENTARY METHODS

Mice

All mice were obtained from The Jackson Laboratories (Bar Harbor, ME, USA). Ischemia-reperfusion (IR) injury was induced in 10- to 12-week-old male C57BL/6J WT mice, in female C57BL/6J WT mice transplanted with BM from male transgenic GFP-expressing (C57BL/6-Tg[CAG-eGFP]1Osb/J) mice, in female C57BL/6J WT mice transplanted with BM from male eNOS-KO (B6.129P2-Nos3^{tm1Unc}/J) mice, in female eNOS-KO mice transplanted with BM from male C57BL/6J WT mice, in female C57BL/6J WT mice transplanted with BM from male C57BL/6J WT mice, in female FVB WT mice transplanted with BM from male Tie-2/GFP transgenic (STOCK Tg[TIE2GFP]287Sato/J) mice, and in male C57BL/6J WT mice or eNOS KO mice that had been intravenously injected with BMPCs from male eNOS-KO mice or C57BL/6J WT mice. Experiments in the absence of IR were performed with 10- to 12-week-old, male C57BL/6J WT mice. All surgical procedures and animal care protocols were approved by the Northwestern University Animal Care and Use Committee.

Bone-marrow transplantation

Donor mice were age-matched to recipient mice aged 4-6 weeks. The transplantation procedure was performed as described previously.[1,2] Briefly, the bone marrow of recipient mice was ablated with radiation (12.0 Gy for C57BL/6J mice and 9.0 Gy for FVB mice), then 5 x 10^6 donor bone-marrow cells were injected intravenously, and the transplanted bone marrow was allowed to regenerate for 6-8 weeks before subsequent experimental procedures were performed.

IR injury model and treatment

IR injury was induced as described previously.[3] Briefly, mice were anesthetized, orally intubated, placed in a supine position on a warm circulating water pad covered with a sterile drape, and a left thoracotomy was performed in the fourth intercostal space;

respiration was controlled with a mechanical rodent ventilator (Nemi Scientific, Inc., Framingham, MA) (tidal volume 0.4 mL, rate 100 strokes/min). The pericardium was removed, and a curved tapered needle was used to pass an 8-0 monofilament nylon suture under the LAD artery just proximal to the first diagonal branch. To secure the occlusion without damaging the artery, the suture was tightened over a polyethylene bar that had been placed on the LAD. Ischemia was verified by epicardial cyanosis, and the occlusion was maintained for 60 minutes before reperfusion while anesthesia was maintained via intraperitoneal administration of tribromoethanol every 20 minutes. Reperfusion was induced by removing the polyethylene bar and verified by epicardial hyperemia; then, the suture was left in place, the chest was closed, and treatment was administered. Mice received a single subcutaneous injection of AMD3100 (5 mg/kg, 125 ug in 100 uL; Sigma-Aldrich Co, St. Louis, MO) or an equal volume of saline.

AAR and infarct area

Animals were anesthetized and intubated for mechanical ventilation; then, a left thoracotomy was performed in the fourth intercostal space and a 7-0 silk suture was inserted around the pulmonary artery and aorta. The LAD artery was re-occluded for 5 minutes by tightening the suture used for the induction of IR injury; then, the suture around the pulmonary artery and aorta was briefly tightened, and 750,000 microspheres (15-um diameter; STERIspheres, BioPal, Worcester, MA, USA) were injected into the LV through the apex. Five minutes later, the heart was arrested by injecting 0.15 mL of 100 mM cadmium chloride into the right ventricle, excised, placed in an agarose-containing well, and cut into 8-12 500-um transverse sections. The sections were stained for 10 minutes at 37°C in wells containing 1.5% triphenyltetrazolium chloride (TTC) solution and digitally photographed under a dissecting microscope. Areas of viable tissue were stained deep red, the AAR was identified by the lack of microspheres (which appeared as blue-gray dots, when present), and the infarcted area remained colorless. For each mouse, the AAR, the area of the infarct, and the area of the LV were quantified via computerized planimetry (ImageJ: NIH Image); AAR was presented as a

percentage of the area of the entire LV, and the infarct area was presented as a percentage of the AAR.

BM MMP-9 and sKitL protein levels

Bone marrow plasma was collected by flushing femurs and tibias with 0.5 mL of PBS and then centrifuged for 20 minutes at 2,000 g and 4ºC and for 10 minutes at 10,000 g and 4ºC. Supernatant levels of MMP-9 and sKitL were measured by ELISA (R&D Systems, Minneapolis, MN USA).[4]

PB cell counts

Blood (150 uL) was collected from the orbital veins of anesthetized mice. Total PB MNC counts were measured by determining the number of lymphocytes and monocytes in 10 uL of the blood sample with a HemaVet Mascot Multispecies Hematology System Counter 1500 R (CDC Technologies Inc., Oxford, CT). For FACS analyses, MNCs were isolated from the remaining sample via gradient-density centrifugation with Histopaque-1083 (Sigma- Aldrich Corp.) as described previously[3] and labeled with FITC-conjugated anti-mouse Sca1 antibodies, PE-conjugated anti-mouse Flk1 antibodies, and APC-conjugated anti-mouse CXCR4 antibodies (BD Pharmingen Inc, San Diego, CA, USA); then, the number of sca1+/flk1+ MNCs and CXCR4+ MNCs in the MNC fraction was determined with a Dako Cytomation CyAn flowcytometer and Flow-Jo Software (Tree Star, Inc., Ashland, OR, USA). Isotype-matched IgG antibodies (Jackson ImmunoResearch Laboratories Inc., West Grove, PA, USA) were used as negative controls, and 100,000 events were counted per sample.[5] MNCs positive for both Sca1 and Flk1 expression were considered BMPCs, and PB cell counts were calculated by multiplying the total PB MNC count by the proportion of positively-stained cells in the MNC fraction. For the BMPC culture assay, MNCs were isolated from 500 uL of PB via density gradient centrifugation and cultured for 4 days in supplemented EBM-2 (Lonza Walkersville Inc., Walkersville, MD, USA) medium containing 5% FBS (SingleQuot Kit; Lonza Walkersville Inc.) on 4-well glass chamber slides that had been coated with rat vitronectin (Sigma-Aldrich Corp.) in 0.1% gelatin; then, the cells were incubated with DiI-

acLDL (Biomedical Technologies Inc., Stoughton, MA, USA) for 2 hours and stained with FITC-conjugated BS1 lectin (Vector Laboratories, Burlingame, CA, USA). Spindle-shaped cells positive for both acLDL and BS1 lectin were considered BMPCs and counted in 10 randomly selected HPFs (20x).

Recruitment of systemically injected BMPCs

Seven days before the induction of IR injury, mice were splenectomized as previously reported[6] via vessel ligation through a lateral incision in the left abdominal wall. BMPCs were isolated from WT and eNOS-knockout mice, cultured for 6 days, and labeled with DiI-acLDL for 2 hours before injection. BMPCs ($5x10^5$ per mouse) were injected intravenously 24 hours after IR injury was induced, and mice were sacrificed 48 hours later (i.e., 3 days after IR injury).

NO Production

The concentration of nitrate and nitrite (i.e., the final metabolites of NO) was determined with a Nitrate/Nitrite Colorimetric Assay Kit (Cayman Chemical, Ann Arbor, MI, USA) as directed by the manufacturer's instructions and reported as the optical density at 540 nm wavelength. PB measurements were performed with serum from 500 µL of blood that had been collected from the heart and centrifuged (1500 rpm, 4°C) for 15 minutes. For measurements in cultured cells, BMPCs were cultured in EBM-2 medium containing 5% FBS, or in EBM-2/FBS medium containing 10 uM AMD3100 for 48 hours at 37°C.

Histological and immunofluorescent assessments

Histological assessments were performed in frozen or paraffin-embedded sections. To prepare frozen bone sections, explanted bones were fixed with 4% paraformaldehyde for 5 hours, decalcified with 10% EDTA for 72 hours, and washed with 30% sucrose solution overnight. For frozen heart sections, hearts were washed with PBS delivered through both the right and left ventricle before excision and with PBS delivered through the aorta after excision; then, the coronary artery was perfused with 4% PFA delivered through the aorta, and hearts were kept in 4% PFA for 5 hours and in 30% sucrose

solution overnight. Bone and heart samples were embedded in OCT compound (Sakura Finetek U.S.A., Inc., Torrance, CA, USA), snap-frozen in liquid nitrogen, and cut into sections.

To prepare paraffin-embedded sections, the abdominal aorta was cannulated with a polyethylene catheter, and 1 mL of heparin/PBS solution (100 IU/mL heparin, 0.2 M PBA, pH 7.4) was injected; then, 0.15 mL of 100 mM cadmium chloride was injected through the catheter to arrest the heart in diastole, the thorax was opened, the heart was perfused at mean arterial pressure with phosphate-buffered formalin, the right atrium was cut to allow drainage, and fixative was delivered through a 25 G3/4 Vacutainer (BD, Franklin Lakes, NJ, USA) that had been inserted into the left ventricle. At the end of the procedure, the whole heart was excised (beginning at the ascending aorta), embedded in paraffin, and cut into sections.

Fibrosis

Fibrosis was evaluated in paraffin-embedded, Masson-trichrome–stained heart sections with a computerized digital image analysis system (ImageJ: NIH image) and reported as the ratio of the length of fibrosis to the left-ventricular circumference.

Capillary density

Capillaries were identified by injecting mice with BS-1 lectin (Vector Laboratories) 10 minutes before sacrifice, and then staining paraffin-embedded sections with anti-lectin primary antibodies (Vector Laboratories) and Alexa 555-conjugated anti-goat IgG secondary antibodies (Invitrogen, Carlsbad, CA, USA). Capillary density was evaluated by counting positively stained tubular structures in 3 sections, 3 high-power fields (HPFs) per section.

BM-derived cell incorporation

BM-derived cells were identified in the hearts of female WT mice transplanted with BM from male GFP-expressing mice by staining paraffin-embedded sections with anti-

mouse GFP primary antibodies (Invitrogen) and Alexa 488-conjugated anti-goat IgG secondary antibodies (Invitrogen). Positively stained cells were counted in 3 sections, 3 HPFs per section.

eNOS expression

eNOS-expressing cells were identified by staining frozen bone sections and paraffin-embedded heart sections with anti-NOS3 primary antibodies (Santa Cruz Biotechnology, Inc., Santa Cruz, CA, USA) and Alexa 555-conjugated anti-rabbit IgG secondary antibodies (Invitrogen). Positively stained cells were counted in 3 sections, 3 HPFs per section.

Apoptosis

Cells with fragmented nuclear DNA were identified in paraffin-embedded heart sections via the terminal deoxynucleotide transferase-mediated dUTP nick end labeling (TUNEL) method (Roche Molecular Biochemicals, Mannheim, Germany) followed by DAPI staining. Positively stained cells were counted in 4 sections, 3 HPFs per section.

In vitro assessments with cultured, bone marrow-derived progenitor cells

Cell collection and enrichment

BM cells were collected by flushing mouse tibias and femurs with 3 mL of 5 mM EDTA in PBS; then, BM MNCs were isolated from the total BM cell population by density gradient centrifugation with Histopaque-1083 (Sigma-Aldrich Corp.) as described previously,[3] plated ($5x10^5$ cells per cm^2) on RepCell® culture dishes coated with rat vitronectin, and cultured in EBM-2 medium containing 10% FBS. Four days later, non-adherent cells were washed away and adherent cells were detached by leaving the plates at room temperature for 30 minutes. The detached cells were re-seeded on vitronectin-coated plates and cultured in fresh EBM-2/FBS medium for 2 days before subsequent experiments were performed.

mRNA expression

BMPCs were treated with 10 uM AMD3100 in EBM-2 medium containing 5% FBS or with EBM-2/FBS medium alone for 6 hours at 37°C; then, mRNA expression was evaluated via quantitative RT-PCR.

Quantitative real-time RT-PCR

Total RNA was extracted from cultured cells with a QIAamp RNA blood mini Kit (QIAGEN Inc.) and from homogenized heart tissue with RNA STAT-60 (Tel-Test, Inc.) as directed by the manufacturers' instructions. The RNA was reverse transcribed with a Taqman cDNA Synthesis Kit (Applied Biosystems) and amplified on a Taqman 7500 (Applied Biosystems); primer and probe sequences are listed in the Supplementary Table 1. Expression was calculated via the comparative threshold cycle (CT) method and normalized to 18S expression.

Luciferase reporter assay

Mouse endothelial cells (sVECs) were co-transfected with a luciferase reporter construct coding for the eNOS promoter (eNOS-Luc, generated by SwitchGear Genomics, Menlo Park, CA, USA) and with a pCMVnlacZ plasmid coding for β-galactosidase; transfection was performed with TransFast transfection reagent (Promega Corporation, Madison, WI, USA) as directed by the manufacturer's instructions. Twenty-four hours after transfection, cells were starved overnight and treated with 0 μM, 1 μM, 10 μM, or 100 μM AMD3100 for 18 hours; then, luciferase activity was measured with a Luciferase System (Promega) and β-galactosidase activity was assayed as previously described.[7] For each sample, luciferase activity was normalized to β-galactosidase activity to compensate for differences in transfection efficiency. Each condition was assayed in triplicate, and each experiment was performed at least three times.

SUPPLEMENTARY REFERENCES

1. Asahara T, Masuda H, Takahashi T, Kalka C, Pastore C, Silver M, Kearne M, Magner M, Isner JM. Bone marrow origin of endothelial progenitor cells

responsible for postnatal vasculogenesis in physiological and pathological neovascularization. *Circ Res*. 1999;85:221-228.

2. Asahara T, Takahashi T, Masuda H, Kalka C, Chen D, Iwaguro H, Inai Y, Silver M, Isner JM. VEGF contributes to postnatal neovascularization by mobilizing bone marrow-derived endothelial progenitor cells. *Embo J*. 1999;18:3964-3972.
3. Ii M, Nishimura H, Iwakura A, Wecker A, Eaton E, Asahara T, Losordo DW. Endothelial progenitor cells are rapidly recruited to myocardium and mediate protective effect of ischemic preconditioning via "imported" nitric oxide synthase activity. *Circulation*. 2005;111:1114-1120.
4. Aicher A, Heeschen C, Mildner-Rihm C, Urbich C, Ihling C, Technau-Ihling K, Zeiher AM, Dimmeler S. Essential role of endothelial nitric oxide synthase for mobilization of stem and progenitor cells. *Nat Med*. 2003;9:1370-1376.
5. Iwakura A, Shastry S, Luedemann C, Hamada H, Kawamoto A, Kishore R, Zhu Y, Qin G, Silver M, Thorne T, Eaton L, Masuda H, Asahara T, Losordo DW. Estradiol enhances recovery after myocardial infarction by augmenting incorporation of bone marrow-derived endothelial progenitor cells into sites of ischemia-induced neovascularization via endothelial nitric oxide synthase-mediated activation of matrix metalloproteinase-9. *Circulation*. 2006;113:1605-1614.
6. Hamada H, Kim MK, Iwakura A, Ii M, Thorne T, Qin G, Asai J, Tsutsumi Y, Sekiguchi H, Silver M, Wecker A, Bord E, Zhu Y, Kishore R, Losordo DW. Estrogen receptors alpha and beta mediate contribution of bone marrow-derived endothelial progenitor cells to functional recovery after myocardial infarction. *Circulation*. 2006;114:2261-2270.
7. Renault MA, Roncalli J, Tongers J, Misener S, Thorne T, Jujo K, Ito A, Clarke T, Fung C, Millay M, Kamide C, Scarpelli A, Klyachko E, Losordo DW. The Hedgehog transcription factor Gli3 modulates angiogenesis. *Circ Res*. 2009;105:818-826.

SUPPLEMENTARY TABLES.

Supplementary Table 1. *RT-PCR primers and probes.*

Gene	Primer/Probe	Sequence
Mouse eNOS	forward	5’-TCTGCGGCGATGTCACTATG-3’
	reverse	5’-CATGCCGCCCTCTGTTG-3’
	probe	5’-FAM-AACCAGCGTCCTGCAAACCGTGC-BHQ-3’
Mouse SDF-1α	forward	5’-CCTCCAAACGCATGCTTCA-3’
	reverse	5’-CCTTCCATTGCAGCATTGGT-3’
	probe	5’-FAM-CTGACTTCCGCTTCTCACCTCTGTAGCCT-BHQ-3’

Supplementary Table 2. *Echocardiographic parameters. (dimensional values at each time point)*

	Time	Treatment	LVDd (mm)		LVDs (mm)		FS (%)	
			AVERAGE	STDEV	AVERAGE	STDEV	AVERAGE	STDEV
Intact mouse	day 0	pre treatment	3.60	0.44	2.02	0.35	44.22	3.38
	day 7	Saline	3.20	0.70	2.05	0.75	37.07	9.24
		AMD	3.10	0.40	1.91	0.42	38.68	7.75
	day 14	Saline	3.39	0.68	2.34	0.79	32.35	9.07
		AMD	3.20	0.51	2.03	0.48	37.06	7.73
	day 28	Saline	3.14	0.46	2.21	0.46	29.88	7.06
		AMD	3.15	0.28	2.09	0.37	33.64	9.30
WT BM to WT recip	day 0	pre treatment	3.70	0.50	2.52	0.58	32.49	6.86
	day 7	Saline	4.13	0.61	3.08	0.57	25.73	3.03
		AMD	3.50	0.35	2.71	0.42	22.90	6.10
	day 14	Saline	2.91	0.07	2.28	0.13	21.79	3.25
		AMD	3.41	0.10	2.65	0.14	22.28	2.41
	day 28	Saline	3.37	0.25	2.78	0.32	17.81	3.74
		AMD	3.55	0.19	2.79	0.11	21.46	1.19
eNOS KO BM to WT recip	day 0	pre treatment	4.08	0.61	2.99	0.63	29.14	3.12
	day 7	Saline	3.59	0.42	2.79	0.59	22.74	8.07
		AMD	3.80	0.01	2.83	0.25	25.55	6.66
	day 14	Saline	3.19	0.23	2.51	0.20	21.23	1.86
		AMD	3.79	0.20	2.95	0.10	22.13	1.46
	day 28	Saline	3.52	0.14	2.84	0.20	19.18	5.41
		AMD	3.79	0.20	2.95	0.10	22.13	1.46
WT BM to eNOS KO recip	day 0	pre treatment	3.39	0.32	2.26	0.44	33.63	8.83
	day 7	Saline	3.25	0.45	2.46	0.42	24.48	5.65
		AMD	3.01	0.43	2.19	0.51	28.00	8.32
	day 14	Saline	3.49	0.19	2.95	0.27	15.40	3.73
		AMD	3.44	0.18	2.71	0.30	21.31	6.36
	day 28	Saline	3.75	0.27	3.30	0.47	12.22	6.16
		AMD	3.35	0.73	2.60	0.91	23.97	10.97
EPC injection therapy	day 0	pre treatment	3.80	0.18	2.45	0.16	35.48	1.56
	day 7	Saline	3.65	0.42	2.96	0.63	19.67	7.94
		WT EPCs	3.67	0.35	2.72	0.51	26.39	7.18
		eNOS KO EPCs	3.77	0.14	2.89	0.26	23.51	4.89
	day 14	Saline	4.29	0.32	3.53	0.33	17.79	1.54
		WT EPCs	3.90	0.51	3.07	0.27	21.04	3.71
		eNOS KO EPCs	4.00	0.19	3.12	0.23	22.22	3.18
	day 28	Saline	4.11	0.14	3.41	0.22	17.16	4.56
		WT EPCs	4.09	0.39	3.23	0.39	21.02	3.35
		eNOS KO EPCs	4.27	0.29	3.27	0.48	23.30	10.12

Supplementary Table 3. *Echocardiographic parameters (p values compared to baseline) corresponding to Figure 1F, G and H.*

		Day 7	Day 14	Day 28
LV FS	Saline	0.0001	<0.0001	<0.0001
	AMD	0.0006	0.0005	0.0002
LV As	Saline	0.073	0.0058	0.0001
	AMD	0.368	0.134	0.0074
LV Ad	Saline	0.485	0.087	0.013
	AMD	0.742	0.139	0.04

LV indicates left ventricule, FS; fractional shortening, As; area at end-systolic phase, Ad; area at end-diastolic phase.

Supplementary Figure 1

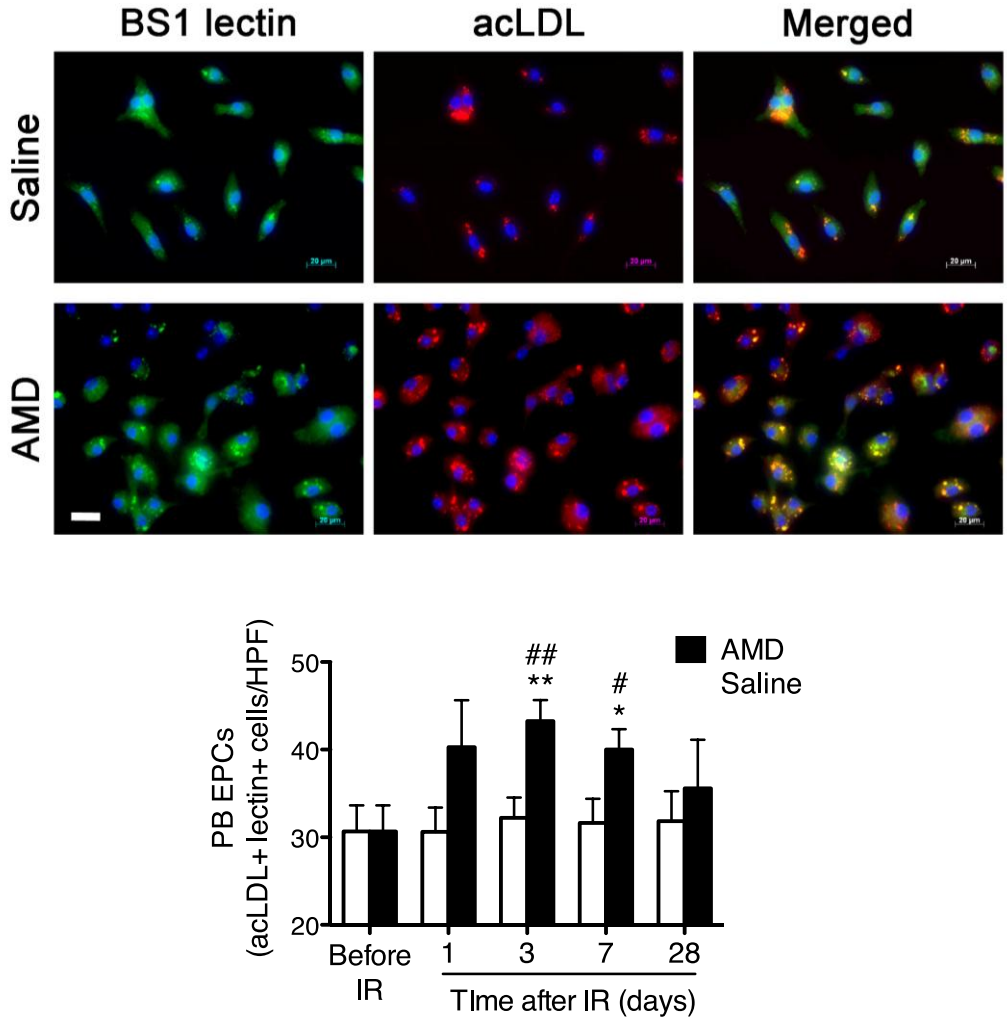

Supplementary Figure 1. AMD3100 enhances BMPC mobilization after IR injury. Circulating BMPC levels were determined in mice before IR injury and treatment with AMD3100 or saline and from 1-28 days afterward via the BMPC culture assay. MNCs were isolated from the PB, cultured for 4 days, then stained with fluorescent anti-BSl lectin (green) and anti-acLDL (red) antibodies; nuclei were counterstained with DAPI (blue). BMPC levels were quantified as the number of cells stained positively for both BS1 lectin and acLDL. Scale bar=20 um.; *P<0.05 and **P<0.01 versus saline. $^{\#}$P<0.05 and $^{\#\#}$P<0.01 versus before IR. n=11-12 per treatment group at each time point.

Supplementary Figure 2

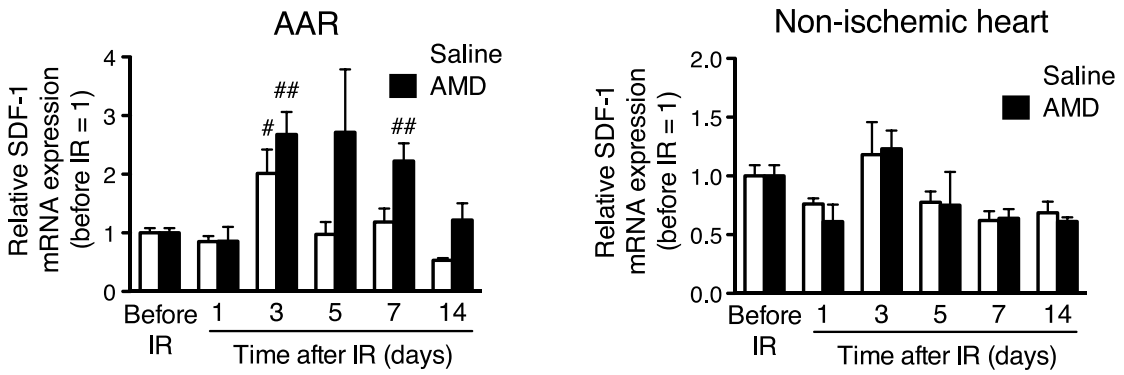

Supplementary Figure 2. AMD3100 increases SDF-1 expression in the AAR after IR injury. SDF-1 mRNA expression was evaluated before IR injury and treatment with AMD3100 or saline and from 1-14 days afterward; assessments were performed both in the AAR and in non-ischemic tissues via quantitative RT-PCR, normalized to 18S rRNA levels, and presented relative to the level of expression before injury. $^{\#}P<0.05$ and $^{\#\#}P<0.01$ versus before IR. n=3-5 per treatment group at each time point.

Supplementary Figure 3

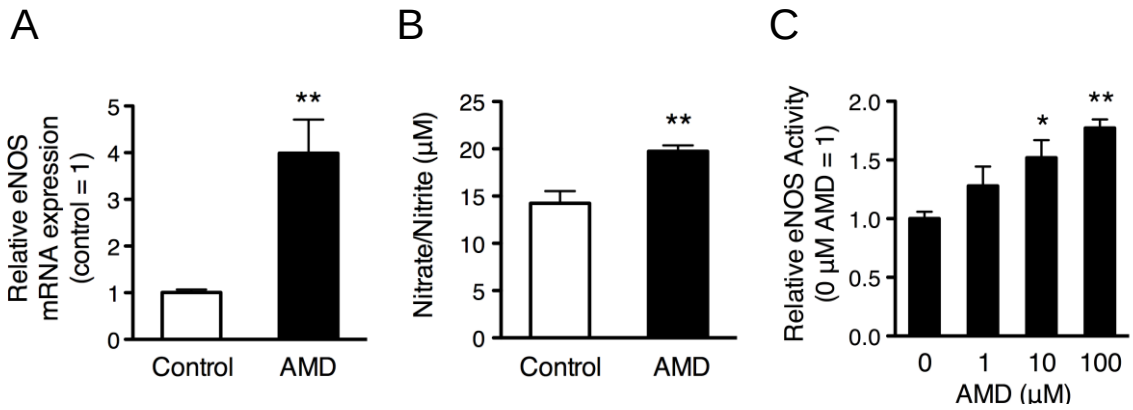

Supplementary Figure 3. AMD3100 increases eNOS activity in BMPCs and endothelial cells. (A, B) 4-day cultured BM MNCs from the BM of WT mice further cultured with (AMD) or without (Control) 10 uM AMD3100 for 6 hours. (A) eNOS mRNA expression was evaluated via quantitative RT-PCR, normalized to 18S rRNA levels, and presented relative to the level of expression in Control cells. (B) The concentration of nitrate and nitrite (i.e., the final metabolites of NO) in the culture media was determined via a colorimetric assay. (C) Murine endothelial cells were co-transfected with a plasmid coding for luciferase expression from the eNOS promoter and with a plasmid coding for β-galactosidase expression; then, the cells were treated with 0 μM, 1 μM, 10 μM, or 100 μM AMD3100 for 18 hours. eNOS activity was quantified as the ratio of luciferase activity to β-galactosidase activity and presented relative to the level of expression in cells treated with 0 μM AMD3100. *P<0.05 and **P<0.01 versus control (AMD 0μM). n=3-6 per condition for each experiment.

Supplementary Figure 4

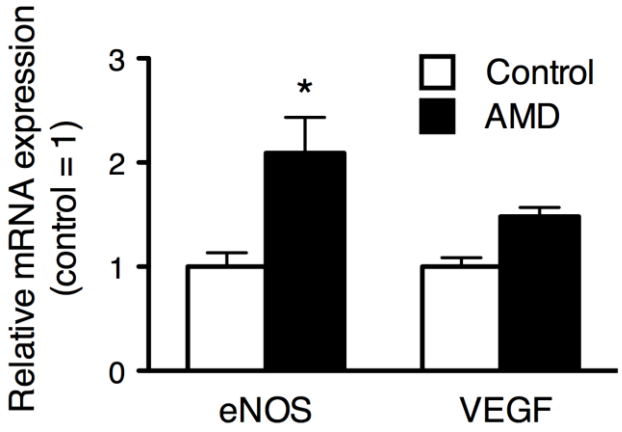

Supplementary Figure 4. AMD3100 increases eNOS but not VEGF activity in BMPCs. 4-day cultured BM MNCs from the BM of WT mice further cultured with (AMD) or without (Control) 10 uM AMD3100 for 6 hours. eNOS and VEGF mRNA expression was evaluated via quantitative RT-PCR, normalized to 18S rRNA levels, and presented relative to the level of expression in Control cells. *P<0.05 versus control. n=3 per condition for each group.